European Radiology (2019) 29:5673–5681
https://doi.org/10.1007/s00330-019-06107-w

MUSCULOSKELETAL

CT temporal subtraction improves early detection of bone metastases compared to SPECT

Koji Onoue[1] · Mizuho Nishio[1,2] · Masahiro Yakami[1,2] · Gakuto Aoyama[3] · Keita Nakagomi[3] · Yoshio Iizuka[3] · Takeshi Kubo[1] · Yutaka Emoto[4] · Thai Akasaka[1] · Kiyohide Satoh[3] · Hiroyuki Yamamoto[3] · Hiroyoshi Isoda[1,2] · Kaori Togashi[1]

Received: 20 August 2018 / Revised: 5 February 2019 / Accepted: 12 February 2019 / Published online: 19 March 2019

Abstract

Objectives To compare observer performance of detecting bone metastases between bone scintigraphy, including planar scan and single-photon emission computed tomography, and computed tomography (CT) temporal subtraction (TS).

Methods Data on 60 patients with cancer who had undergone CT (previous and current) and bone scintigraphy were collected. Previous CT images were registered to the current ones by large deformation diffeomorphic metric mapping; the registered previous images were subtracted from the current ones to produce TS. Definitive diagnosis of bone metastases was determined by consensus between two radiologists. Twelve readers independently interpreted the following pairs of examinations: NM-pair, previous and current CTs and bone scintigraphy, and TS-pair, previous and current CTs and TS. The readers assigned likelihood levels to suspected bone metastases for diagnosis. Sensitivity, number of false positives per patient (FPP), and reading time for each pair of examinations were analysed for evaluating observer performance by performing the Wilcoxon signed-rank test. Figure-of-merit (FOM) was calculated using jackknife alternative free-response receiver operating characteristic analysis.

Results The sensitivity of TS was significantly higher than that of bone scintigraphy (54.3% vs. 41.3%, $p = 0.006$). FPP with TS was significantly higher than that with bone scintigraphy (0.189 vs. 0.0722, $p = 0.003$). FOM of TS tended to be better than that of bone scintigraphy (0.742 vs. 0.691, $p = 0.070$).

Conclusion Sensitivity of TS in detecting bone metastasis was significantly higher than that of bone scintigraphy, but still limited to 54%. TS might be superior to bone scintigraphy for early detection of bone metastasis.

Key Points

- *Computed tomography temporal subtraction was helpful in early detection of bone metastases.*
- *Sensitivity for bone metastasis was higher for computed tomography temporal subtraction than for bone scintigraphy.*
- *Figure-of-merit of computed tomography temporal subtraction was better than that of bone scintigraphy.*

Keywords Bone · Neoplasm metastasis · Multidetector computed tomography · Scintigraphy · Image processing, computer-assisted

Electronic supplementary material The online version of this article (https://doi.org/10.1007/s00330-019-06107-w) contains supplementary material, which is available to authorized users.

✉ Mizuho Nishio
nmizuho@kuhp.kyoto-u.ac.jp; nishio.mizuho.3e@kyoto-u.jp

[1] Department of Diagnostic Imaging and Nuclear Medicine, Kyoto University Graduate School of Medicine, 54 Kawahara-cho, Shogoin, Sakyo-ku, Kyoto 606-8507, Japan

[2] Preemptive Medicine and Lifestyle-related Disease Research Center, Kyoto University Hospital, 53 Kawahara-cho, Shogoin, Sakyo-ku, Kyoto 606-8507, Japan

[3] Medical Imaging System Development Center, R&D Headquarters, Canon Inc., 30-2, Shimomaruko 3-chome, Ohta-ku, Tokyo 146-8501, Japan

[4] Kyoto College of Medical Science, 1-3 Imakita, Koyamahigashi-cho, Sonobe-cho, Nantan, Kyoto 622-0041, Japan

Abbreviations

^{18}F-FDG-PET	^{18}F-fluoro-2-deoxy-d-glucose positron emission tomography
CT	Computed tomography
FOM	Figure-of-merit
JAFROC	Jackknife free-response receiver operating characteristic
LDDMM	Large deformation diffeomorphic metric mapping
MRI	Magnetic resonance imaging
NM	Nuclear medicine
SPECT	Single-photon emission computed tomography
TS	CT temporal subtraction

Introduction

In addition to lung and liver, bones are one of the most common sites for metastasis [1]. Bone metastases are associated with various complications, such as pain and bone destruction. Vertebral metastases, in particular, can cause compression fractures and neural disturbances, such as quadriplegia, which can consequently deteriorate the patients' quality of life [1–4]. Owing to advancements in anticancer treatments, complications associated with bone metastases can be reduced [1–5]. However, detection of bone metastases at an early stage remains a fundamental step in anticancer treatment. Therefore, clinical follow-up of patients with cancer is a crucial step for preventing various complications through early and accurate detection of bone metastases.

Computed tomography (CT) is used as the primary modality for examining local recurrence and distant metastases during clinical follow-up. Recent high-resolution multi-detector CT images provide a huge amount of anatomical information. Consequently, substantial effort by radiologists is required for detecting bone metastases on these CT images. There are several helpful diagnostic imaging methods other than CT for detecting bone metastases: planar scan and single-photon emission computed tomography (SPECT) of ^{99m}Tc bone scintigraphy, magnetic resonance imaging (MRI), ^{18}F-fluoro-2-deoxy-d-glucose positron emission tomography (^{18}F-FDG-PET), and ^{18}F-sodium fluoride PET [6–16]. However, it is important to note that these diagnostic imaging methods are not routinely performed during the follow-up of patients with cancer and without typical symptoms. Among these methods, bone scintigraphy has been frequently used for detection of bone metastases [13]. According to previous studies, sensitivity of ^{18}F-FDG-PET is superior for osteolytic and inferior for osteoblastic metastasis to that of bone scintigraphy [12, 14, 15], because the tracer uptake of bone scintigraphy for osteoblastic metastasis is higher than that for osteolytic one [14].

A previous study showed that CT temporal subtraction (TS) improved a radiologist's performance in detecting newly developed bone metastases during serial follow-up CT [17]. Another study also showed that TS was useful for detecting vertebral metastases regardless of the metastasis being osteolytic or osteoblastic [18]. These results suggest that TS is a promising tool for detecting bone metastasis.

One of the reasons for difficulty in detecting bone metastasis on CT images is that the CT density of the bone is higher than that of other organs. Therefore, changes in the CT density due to bone metastases are not clearly depicted on CT images. Bone window condition, characterised by wide window width and high window level, is usually applied to CT images for bone viewing. However, its application hinders detection of subtle changes in bone CT density. Because bones without temporal changes have no signal on TS images, TS can clearly depict temporal changes due to bone metastasis.

To the best of our knowledge, no studies have compared the detectability of bone metastasis between TS and bone scintigraphy. Hence, the aim of our study was to compare the observer performances of detecting bone metastases between bone scintigraphy and TS using large deformation diffeomorphic metric mapping (LDDMM) [19, 20].

Materials and methods

The authors received approval from ethics committee of Kyoto university graduate school and faculty of medicine and Kyoto university hospital. Informed consent was waived because this was a retrospective study using CT, bone scintigraphy, and clinical examination results.

Inclusion criteria and lesion confirmation

Sixty consecutive patients with cancer were selected from our clinical database between February 2008 and March 2016. Thirty bone-metastasis-positive and 30 bone-metastasis-negative patient records were included. We selected these 60 records according to the following inclusion criteria: (i) history of malignancy, (ii) availability of CT images at three time points (previous, current, and future CT), (iii) the three CT examinations covered the whole body (i.e. chest-to-pelvis), and (iv) both planar scan and SPECT of bone scintigraphy were available within 2 months of the current CT.

The following criteria were used as the definition of a newly developed bone metastasis: (i) bone metastases emerged or enlarged after the previous CT; (ii) bone metastasis was confirmed on the current CT, bone scintigraphy, or both; and (iii) bone metastasis was confirmed on the future CT.

The inclusion criterion for the 30 bone-metastasis-positive patient records was that the number of newly developed bone metastases (size > 5 mm) was ≤ 10. The inclusion criterion for the 30 bone-metastasis-negative patient records was no

perceptible bone metastases on the previous, current, or future CTs or bone scintigraphy.

These criteria were confirmed by consensus between two radiologists (KO and MN with 7 and 11 years of experience, respectively) who did not participate in the following observer study. Definitive determination of bone metastasis location was done by consensus between the two radiologists after examining the three sets of CT images and all available clinical information and imaging data including symptoms, laboratory data, CT, TS, bone scintigraphy, ^{18}F-FDG-PET/CT, and MRI.

CT scans

All CT scans were performed using multi-detector CT scanners. Details of the CT scan are described in Supplementary Material 1. Use of the intravenous contrast medium varied according to the patients' diseases or clinical status. We used non-contrast-enhanced CT images or late-phase contrast-enhanced CT images in our study.

Bone scintigraphy

Planar scan and SPECT of bone scintigraphy were performed within 3 h of administration of 555 MBq of ^{99m}Tc-hydroxymethylene diphosphonate using Gamma-cameras (Infinia GP3; GE Healthcare), which obtained step-and-shoot scans (150 s/bed, total 5–6 beds). The scan time was approximately 30 min. The matrix sizes of the planar image and SPECT of bone scintigraphy were 256 × 1024 and 128 × 128 pixels, respectively. The field of view of SPECT of bone scintigraphy was 56.6 cm.

Temporal subtraction method

The previous CT images were registered to the current CT images using LDDMM. The TS images were produced by subtracting the registered previous CT images from the current CT images. The detailed process for obtaining TS image is described in Supplementary Material 1.

Observer study

Twelve readers with 6–25 years of experience as radiologists independently interpreted the following pairs of examinations with an interval of > 1 month: (NM-pair) previous CT, current CT, axial SPECT of bone scintigraphy, and planar image of bone scintigraphy; (TS-pair) previous CT, current CT, axial TS, and projection image of TS (Fig. 1). The projection image enables immediate grasping of the whole area of TS images. We randomly divided the 12 readers into two groups of six readers. Six readers interpreted in the order of NM-pair then TS-pair, and the other six readers interpreted in the order of TS-pair then NM-pair (Fig. A3 of Supplementary Material). The 12 readers evaluated CT images using bone window condition. All the readers had the chance to use the reformatted CT images. These readers' experience for evaluating bone scintigraphy was 6 ± 3 (1–9) years. The readers were asked to identify newly developed bone metastasis by marking locations with the likelihood for newly developed bone metastasis. They were informed of the patients' age, gender, history of anticancer treatment, and clinical diagnosis of the primary malignancy, and blinded to all other clinical data. The minimum of likelihood was 1, which means that the lesion was regarded as almost certainly non-metastasis. The maximum of likelihood was 100, which means that the lesion was regarded as definitively metastasis. Reading time, which was measured by an independent person, was recorded. In addition, the 12 readers were asked to rate confidence level of their interpretation (survey 1: 1, very low; 2, low; 3, moderate; 4, high; and 5, very high) and usefulness of TS or bone scintigraphy (survey 2: 1, useless; 2, not very useful; 3, somewhat useful; 4, very useful; and 5, extremely useful) on a five-point scale for each case. We performed the observer study with monitors for medical use (Radiforce RX440, EIZO).

Statistical analysis

Jackknife free-response receiver operating characteristic (JAFROC) analysis was employed for evaluating the radiologists' performance [21, 22]. To create free-response ROC curves and calculate figure-of-merit (FOM) values, JAFROC software (JAFROC, version 4; http://www.devchakraborty.com/) was used. The analysis was conducted for a random-readers and random-cases model. In addition, lesion-based sensitivity, number of false positives per patient, patient-based sensitivity, and patient-based specificity were evaluated by Wilcoxon signed-rank test. The likelihood level of diagnosis of a metastasis of 50% was considered as the threshold for calculating sensitivity and specificity; a lesion with > 50% likelihood of diagnosis was considered to indicate bone metastasis. The reading time and confidence level were compared between the two sessions using the Wilcoxon signed-rank test. Values of $p < 0.05$ were considered to indicate statistically significant differences.

Results

The characteristics of the patients and bone metastases are summarised in Tables 1 and 2, respectively. A total of 78 bone metastases were identified in the 30 bone-metastasis-positive cases. Primary lesions of these 78 bone metastases were as follows: prostate, 31; breast, 16; lung, 9; and others, 22 (kidney, 9; bladder, 4; colon, 4; rectum, 2; testis, 2; and unknown, 1).

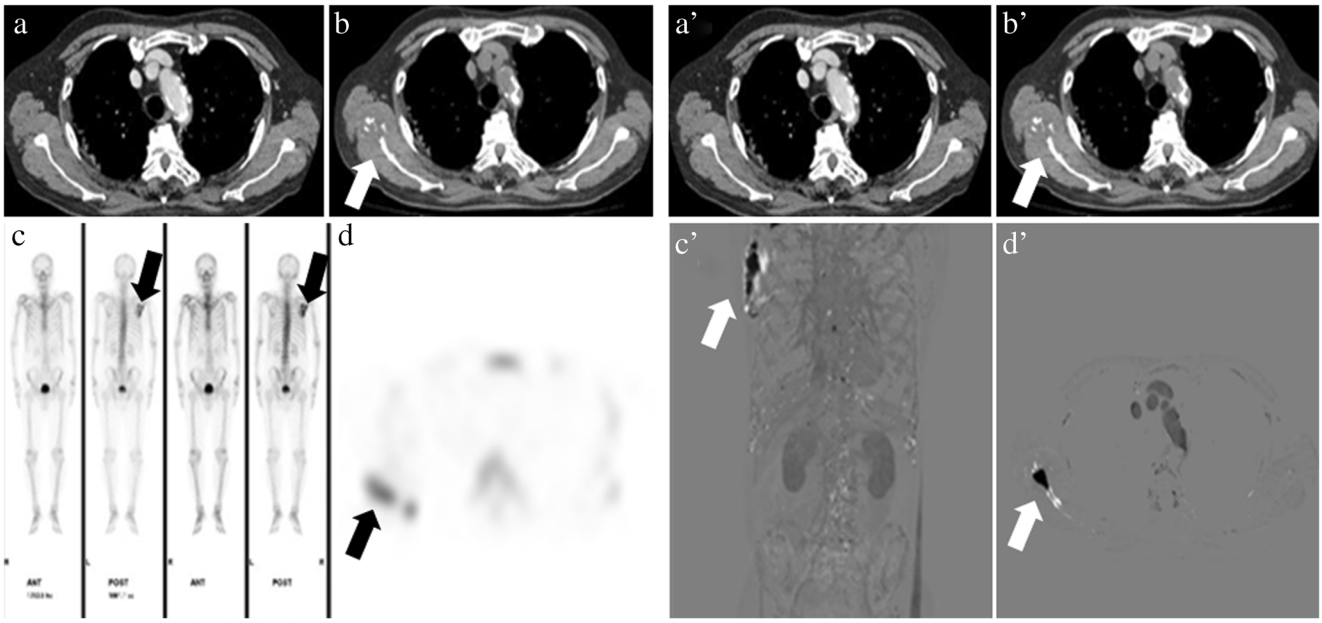

Fig. 1 Representative two pairs of images used in the observer study. A 77-year-old male with osteolytic metastasis of prostate cancer. There is a bone osteolytic metastasis in the right scapula (arrow). On the left side, NM-pair is shown; on the right side, TS-pair is shown. NM-pair comprises (**a**) previous CT image, (**b**) current CT image, (**c**) planar image of scintigraphy, and (**d**) SPECT image of scintigraphy, and TS-pair consists of (**a′**) previous CT image, (**b′**) current CT image, (**c′**) an average of MIP image and MinIP image of TS image, and (**d′**) axial image of TS. Computed tomography (CT), CT temporal subtraction (TS), maximum intensity projection (MIP), minimum intensity projection (MinIP), single-photon emission computed tomography (SPECT)

In this study, there were no registration failures of TS images. According to a previous study [17], the appearance of temporal bone change on TS images varied depending on the type of bone metastases: (i) osteolytic changes were depicted as dark signals on TS images, (ii) osteoblastic changes were depicted as bright signals, and (iii) mixed type changes were depicted as heterogeneous dark and bright signals. As previously described, on TS images in our study, osteolytic, osteoblastic, and mixed type metastases were depicted as dark, bright, and heterogeneous dark and bright signals, respectively (Figs. 2, 3, and 4).

FOM, lesion-based sensitivity, patient-based specificity and sensitivity, number of false positives per patient, reading time, and results of the two surveys by the 12 radiologists are shown in Table 3. The average free-response receiver operating characteristic curves of all 12 readers are shown in Fig. 5. Mean FOM values were 0.691 ± 0.0385 for NM-pair (previous and current CTs and bone scintigraphy) and 0.742 ± 0.0358 for TS-pair (previous and current CTs and TS) ($p = 0.070$). Although FOM of TS-pair tended to be better than that of NM-pair, there was no statistically significant difference. In all but one

Table 1 Characteristics of the subjects in the observer study

		Sixty patients with cancers	Thirty patients with bone metastasis	Thirty patients without bone metastasis
Age (y)		All: 66.0 ± 11.4 (27–85)* Male: 67.8 ± 12.4 (27–85)* Female: 64.3 ± 10.2 (39–80)*	65.6 ± 12.7 (27–84)*	66.4 ± 10.0 (39–85)*
Gender (number of patients)	Male	29	17	12
	Female	31	13	18
Size of bone metastasis (mm)		N/A	17 ± 12 (5–80)*	N/A
Number of bone metastasis per patient		N/A	2.6 ± 1.9 (1–8)*	N/A
Number of patients with anticancer treatment		52	28	24
Mean interval of the paired CT (month)		14.8 ± 9.97 (0.667–55.8)*	16.6 ± 12.4 (0.667–55.8)*	13.1 ± 6.31 (1.60–30.8)*

Not available (N/A)

*Data are shown as mean ± standard deviation and range

Table 2 Characteristics of bone metastasis in the observer study

	Number of bone metastasis				
	Type of bone metastasis			Total	Number of patients
Primary lesion	Osteolytic	Osteoblastic	Osteolytic-osteoblastic mixed		
Prostate	2	29	0	31	12
Breast	0	13	3	16	6
Lung	5	2	2	9	5
Others	13	2	7	22	7
Total	20	46	12	78	30

All 78 bone metastases were larger than 5 mm

radiologist's readings, FOM of TS-pair was higher than that of NM-pair (Table 3).

The lesion-based sensitivity, patient-based sensitivity, patient-based specificity, and number of false positives per patient were 41.3% ± 10.2%, 77.2% ± 8.70%, 95.3% ± 4.61%, and 0.0722 ± 0.0361, respectively, for NM-pair and were 54.3% ± 11.1%, 86.4% ± 7.75%, 90.0% ± 8.50%, and 0.189 ± 0.105, respectively, for TS-pair ($p = 0.006$ for lesion-based sensitivity, $p = 0.004$ for patient-based sensitivity, $p = 0.032$ for patient-based specificity, and $p = 0.003$ for number of false positives per patient). Lesion-based and patient-based sensitivities were higher for TS-pair than for NM-pair with statistical significance. Conversely, the number of false positives per patient was higher for TS-pair than for NM-pair with statistical significance, and the patient-based specificity was higher for NM-pair than for TS-pair with statistical significance.

The median of the readers' confidence in their interpretation (survey 1) was 3 for NM-pair and 4 for TS-pair ($p = 0.059$). The subjective usefulness survey response (survey 2) had a median score of 3 for NM-pair and of 4 for TS-pair ($p = 0.008$). The subjective usefulness survey response of TS-pair was better than that of NM-pair with statistical significance.

The reading time was 208 ± 34.9 s for NM-pair and 187 ± 47.7 s for TS-pair ($p = 0.182$). The reading time of TS-pair tended to be shorter than that of NM-pair. The processing time of the chest-to-pelvis TS images ranged from 40 to 50 min.

Table 4 shows patient-based sensitivity for the primary lesion, and Table 5 shows lesion-based sensitivity for the type of bone metastasis. Supplementary Material 1 shows details of all 30 bone-metastasis-positive cases.

Discussion

This study compared observer performance of detecting bone metastases between bone scintigraphy (planar scan and SPECT) and TS. The results showed that the sensitivity of TS in detecting bone metastases was significantly higher than that of bone scintigraphy. Sakamoto et al compared detectability of newly developed bone metastasis between CT and CT + TS and showed that TS might be useful in detecting bone metastases [17]. Results of the current and previous studies show that CT + TS is potentially useful for efficient detection of bone metastases compared with CT only or CT + bone scintigraphy. The number of false positives per patient with TS was significantly higher than that with bone scintigraphy in the current study. Benign lesions, such as Schmorl nodes, old traumatic lesions, degenerated lesions, and old compression fractures, are generally stable. However, TS was highly sensitive to temporal changes in these benign lesions. Consequently, temporal changes in benign lesions could be misinterpreted as bone metastasis by several radiologists. Overall, based on the results of FOM, detectability of bone metastases by CT + TS tended to be better than that by CT + bone scintigraphy (planar scan + SPECT).

Because TS can be calculated from routinely acquired CT images, TS needs no additional radiation exposure,

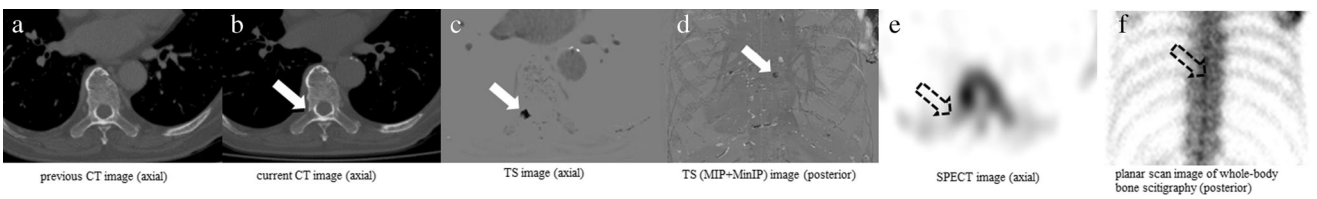

Fig. 2 **a** 77-year-old male with osteolytic metastasis of prostate cancer. There is a bone osteolytic metastasis in the right pedicle (arrow in **b**), and this lesion is depicted clearly as a black region on TS images (arrow in **c**, **d**); however, it is not depicted on scintigraphy images (dotted arrow in **e**, **f**)

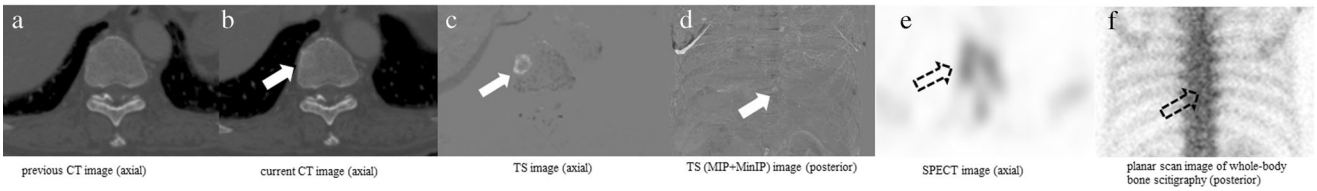

Fig. 3 **a** 69-year-old male with osteoblastic metastasis of prostate cancer. There is a bone osteoblastic metastasis in the vertebral body (arrow in **b**), and this lesion is depicted clearly as a white region on TS images (arrow in **c**, **d**); however, it is not depicted on scintigraphy images (dotted arrow in **e**, **f**)

and costs less than bone scintigraphy. Based on our results, we speculate that, if routinely acquired CT is available, we can substitute bone scintigraphy by routinely acquired CT and TS. Hence, there is a possibility that radiation exposure and costs associated with bone scintigraphy can be reduced. The reasons why detectability of TS is superior to that of bone scintigraphy are the following: first, TS depicts both osteolytic bone metastasis and osteoblastic lesions clearly [17], whereas the sensitivity of bone scintigraphy for detecting osteolytic lesions is relatively lower than for osteoblastic ones [12, 14]; second, TS has higher spatial resolution than bone scintigraphy; therefore, small bone metastases are more likely to be detected by TS than by bone scintigraphy. Generally, diagnostic tools with high sensitivity are suitable for disease detection [23]. Hence, we expect TS to be more useful than bone scintigraphy for early detection of bone metastasis if a CT scan was performed in the past.

According to a previous study [17], the processing time of torso TS images was approximately 6 h using a supercomputer, which is too long in clinical situations. In the current study, we reduced the processing time to 40–50 min with a general-purpose workstation by modifying the software of TS. According to the preliminary results using our in-house software, we expect that the processing time can be reduced to < 10 min with a graphics processing unit.

The lesion-based sensitivity with TS in detecting bone metastasis, which was 54% in the current study, was not satisfactory. However, our results show that the sensitivity with TS was higher than that with bone scintigraphy. These results suggest that it is essentially difficult to detect bone metastases with CT and bone scintigraphy. Even in such a situation, it is speculated that TS is more useful than bone scintigraphy.

Our results showed that FOM of TS was better than that of bone scintigraphy. FOM is based on sensitivity and false positives. FOM results indicated that when detecting bone metastases by TS, the higher sensitivity outweighed the harm of false positives.

The reading time of TS tended to be shorter than that of bone scintigraphy. We speculate that because bone metastasis was more clearly depicted on TS than on current CT images, most radiologists could detect bone metastases on TS with a shorter reading time.

As per Table 4, for most primary lesions, the sensitivity of TS was higher than that of bone scintigraphy. When a primary lesion was breast, the sensitivities of TS and bone scintigraphy were comparable. According to Table 5, the sensitivity of TS was higher than that of bone scintigraphy for all types of bone metastasis. Most of the bone metastases were osteoblastic metastases in breast cancers of the current study (Supplementary Material 1). In general, sensitivity of bone scintigraphy for osteoblastic metastasis is superior to osteolytic metastasis [12, 14]. In addition, effectiveness of TS was relatively low for osteoblastic metastasis, according to Table 5. Because of these factors, it is speculated that sensitivity of TS could be comparable with that of bone scintigraphy for osteoblastic metastasis in breast cancer in this current study.

The survival time of patients with cancer is improving because of the progress in treatment and has led to an increase in the incidence of bone metastasis [24]. Complications of bone metastasis are associated with decrease in activities of daily living and quality of life. To prevent such complications, early detection and treatment of bone metastasis has become more important. Hence, accurate detection of bone metastases during follow-up of patients with cancer is one of the most important tasks in diagnostic imaging. However,

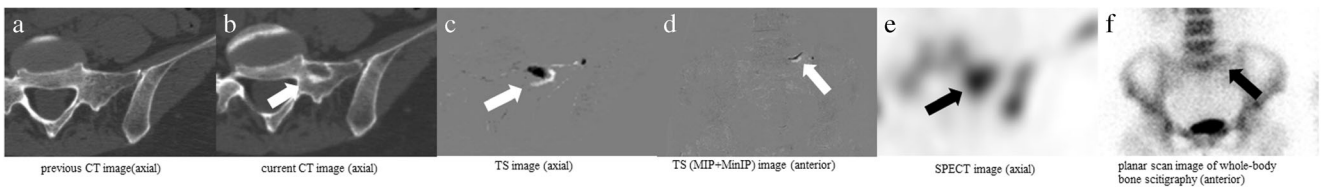

Fig. 4 **a** 52-year-old female with mixed type metastasis of breast cancer. There is mixed type bone metastasis in the left sacrum (arrow in **b**), and this lesion is depicted clearly as a black and white region on TS images (arrow in **c**, **d**); it is depicted clearly on scintigraphy images (black arrow in **e**, **f**)

Table 3 FOM values, lesion-based sensitivities, patient-based sensitivities, patient-based specificities, false positives per patient, reading times, and results of surveys for 12 readers for all cases

Reader	FOM		Lesion-based sensitivity (%)		Patient-based sensitivity (%)		Specificity (%)		False positives per patient		Reading time (sec)		Survey 1 confidence		Survey 2 usefulness	
	NM-pair	TS-pair	NM-pair	TS-pair	NM-pair	TS-pair	NM-pair	TS- pair	NM-pair	TS- pair	NM-pair	TS-pair	NM-pair	TS-pair	NM-pair	TS-pair
1	0.766	0.757	66.7	56.4	86.7	83.3	93.3	96.7	0.0833	0.167	246	214	3	4	5	5
2	0.627	0.664	25.6	39.7	60.0	76.7	96.7	90.0	0.133	0.250	178	164	4	4	4	4
3	0.747	0.796	46.2	66.7	83.3	96.7	96.7	90.0	0.0500	0.0333	174	164	4	4	4	5
4	0.675	0.718	47.4	69.2	83.3	93.3	86.7	66.7	0.100	0.133	279	314	3	3	3	4
5	0.690	0.766	28.2	30.8	60.0	70.0	100	100	0.0333	0.233	213	141	3	3	3	4
6	0.641	0.756	38.5	61.5	76.7	93.3	93.3	90.0	0.0667	0.300	180	173	3	3	3	4
7	0.663	0.689	41.0	44.9	83.3	86.7	93.3	93.3	0.100	0.117	249	133	3	4	3	4
8	0.670	0.738	41.0	59.0	80.0	86.7	96.7	83.3	0.133	0.450	213	235	3	3	3	4
9	0.705	0.755	38.5	47.4	73.3	80.0	100	100	0.0667	0.200	188	180	3	3	3	3
10	0.705	0.734	35.9	60.3	76.7	93.3	100	86.7	0.0333	0.117	179	201	4	4	5	5
11	0.689	0.754	37.2	52.6	76.7	83.3	100	93.3	0.0333	0.100	230	181	3	5	3.5	4
12	0.714	0.782	50.0	62.8	86.7	93.3	86.7	90.0	0.0333	0.167	166	149	3	4	3	5
	Mean												Median			
	0.691	0.742	41.3	54.3	77.2	86.4	95.3	90.0	0.0722	0.189	208	187	3	4	3	4
	Standard deviation															
	0.0385	0.0358	10.2	11.1	8.70	7.75	4.61	8.50	0.0361	0.105	34.9	47.7				

NM-pair: previous and current CTs and bone scintigraphy; TS-pair: previous and current CTs and TS

FOM: Figureof-merit; CT: computed tomography; TS: CT temporal subtraction

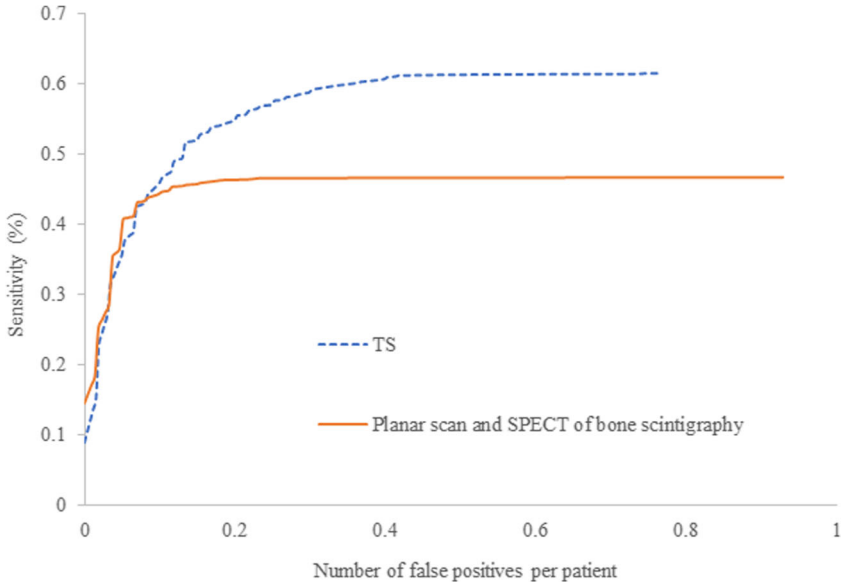

Fig. 5 Average free-response receiver operating characteristic curves. Average free-response receiver operating characteristic curves of TS and bone scintigraphy images. Mean FOM of TS and bone scintigraphy is 0.742 and 0.691, respectively. Computed tomography (CT), CT temporal subtraction (TS), figure-of-merit (FOM), single-photon emission computed tomography (SPECT)

detection of bone metastasis requires substantial effort by radiologists during routine CT scans. Previous studies [17] and our results show that TS obtained from routine CT scans can enhance detectability of bone metastases.

There were several limitations in our study. First, this was a retrospective single-centre study; all data were collected from our clinical database. Second, the bone lesions were not confirmed by histology. In a clinical setting, it is rare to perform a biopsy to obtain histological confirmation of bone metastases when a primary lesion is evident. Third, we evaluated pairs of thin-slice (1 mm) CT images only, whereas a pair of thin-slice CT images is not always available in clinical settings. We expect that advances in CT scanner technology and in the picture archiving and communication system can make TS technology widely available. Fourth, we did not evaluate SPECT/CT of bone scintigraphy. In our observer study, the pairs of images included CT images. We speculate that the diagnostic ability of CT and bone scintigraphy (planar scan and SPECT) together is almost identical to that of CT and SPECT/CT of bone scintigraphy. Fifth, performance evaluations of inexperienced readers were not evaluated and must be investigated in the future. Sixth, we did not evaluate the therapy response of bone metastasis with TS. Under radiotherapy and/or chemotherapy, the density of bone metastasis could be changed on CT images [25]. These changes might be depicted on TS images. Therefore, we might use TS images to determine therapy response of bone metastasis in a future study. Finally, we assumed that CT examinations were routinely performed once or twice a year for patients with cancer. In this clinical situation, TS can potentially reduce costs and radiation exposure associated with bone scintigraphy. If routinely performed CT images are not available, cost of TS is not inexpensive. However, we did not assume such a situation in the current study.

In conclusion, the sensitivity of TS in detecting bone metastasis was significantly higher than that of bone scintigraphy, including planar scan and SPECT, but still limited to 54%. TS might be superior to bone scintigraphy for the early detection of bone metastasis.

Table 4 Patient-based sensitivity for primary lesions

	Patient-based sensitivity (%)	
Primary lesion	Bone scintigraphy	TS
Prostate	73	80
Breast	79	81
Lung	73	88
Others	86	95
Overall	77	86

TS: CT temporal subtraction

Table 5 Lesion-based sensitivity for type of bone metastasis

	Lesion-based sensitivity (%)	
Type of bone metastasis	Bone scintigraphy	TS
Osteoblastic	36	43
Osteolytic	36	63
Mixed	69	85
Overall	41	54

TS: CT temporal subtraction

Funding This research is supported by the Project Promoting Clinical Trials for Development of New Drugs and Medical Devices from Japan Agency for Medical Research and Development, AMED. The funders had no role in study design, data collection and analysis, decision to publish, or preparation of the manuscript.

Compliance with ethical standards

Guarantor The scientific guarantor of this publication is K.Togashi.

Conflict of interest The authors of this manuscript declare relationships with the following companies: Canon Inc. K.Togashi has received research grants from Canon Inc.

Statistics and biometry No complex statistical methods were necessary for this paper.

Informed consent Written informed consent was waived by the Institutional Review Board.

Ethical approval Institutional Review Board approval was obtained.

Methodology
- retrospective
- diagnostic or prognostic study
- performed at one institution

References

1. Yu HH, Tsai YY, Hoffe SE (2012) Overview of diagnosis and management of metastatic disease to bone. Cancer Control 19(2): 84–91
2. Patchell RA, Tibbs PA, Regine WF et al (2005) Direct decompressive surgical resection in the treatment of spinal cord compression caused by metastatic cancer: a randomised trial. Lancet 366(9486):643–648
3. Loblaw DA, Mitera G, Ford M, Laperriere NJ (2012) A 2011 updated systematic review and clinical practice guideline for the management of malignant extradural spinal cord compression. Int J Radiat Oncol Biol Phys 84(2):312–317
4. Bilsky MH, Lis E, Raizer J, Lee H, Boland P (1999) The diagnosis and treatment of metastatic spinal tumor. Oncologist 4(6):459–469
5. Klimo P Jr, Kestle JR, Schmidt MH (2003) Treatment of metastatic spinal epidural disease: a review of the literature. Neurosurg Focus 15(5):E1
6. Palmedo H, Marx C, Ebert A et al (2014) Whole-body SPECT/CT for bone scintigraphy: diagnostic value and effect on patient management in oncological patients. Eur J Nucl Med Mol Imaging 41(1):59–67
7. Damle NA, Bal C, Bandopadhyaya GP et al (2013) The role of 18F-fluoride PET-CT in the detection of bone metastases in patients with breast, lung and prostate carcinoma: a comparison with FDG PET/CT and 99mTc-MDP bone scan. Jpn J Radiol 31(4):262–269
8. Schirrmeister H, Glatting G, Hetzel J et al (2001) Prospective evaluation of the clinical value of planar bone scans, SPECT, and (18)F-labeled NaF PET in newly diagnosed lung cancer. J Nucl Med 42(12):1800–1804
9. Even-Sapir E, Metser U, Mishani E, Lievshitz G, Lerman H, Leibovitch I (2006) The detection of bone metastases in patients with high-risk prostate cancer:99mTc-MDP planar bone scintigraphy, single- and multi-field-of-view SPECT,18F-fluoride PET, and 18F-fluoride PET/CT. J Nucl Med 47(2):287–297
10. Yen RF, Chen CY, Cheng MF et al (2010) The diagnostic and prognostic effectiveness of F-18 sodium fluoride PET-CT in detecting bone metastases for hepatocellular carcinoma patients. Nucl Med Commun 31(7):637–645
11. Tateishi U, Morita S, Taguri M et al (2010) A meta-analysis of (18)F-fluoride positron emission tomography for assessment of metastatic bone tumor. Ann Nucl Med 24(7):523–531
12. Krüger S, Buck AK, Mottaghy FM et al (2009) Detection of bone metastases in patients with lung cancer: 99mTc-MDP planar bone scintigraphy, 18F-fluoride PET or 18F-FDG PET/CT. Eur J Nucl Med Mol Imaging 36(11):1807–1812
13. Delbeke D, Segall GM (2011) Status of and trends in nuclear medicine in the United States. J Nucl Med 52(2):24S–28S
14. Nakai T, Okuyama C, Kubota T et al (2005) Pitfalls of FDG-PET for the diagnosis of osteoblastic bone metastases in patients with breast cancer. Eur J Nucl Med Mol Imaging 32(11):1253–1258
15. Ito S, Kato K, Ikeda M et al (2007) Comparison of 18F-FDG PET and bone scintigraphy in detection of bone metastases of thyroid cancer. J Nucl Med 48(6):889–895
16. Cook GJ, Houston S, Rubens R, Maisey MN, Fogelman I (1998) Detection of bone metastases in breast cancer by 18FDG PET: differing metabolic activity inosteoblastic and osteolytic lesions. J Clin Oncol 16(10):3375–3379
17. Sakamoto R, Yakami M, Fujimoto K et al (2017) Temporal subtraction of serial CT images with large deformation diffeomorphic metric mapping in the identification of bone metastases. Radiology 285(2):629–639
18. Iwano S, Ito R, Umakoshi H et al (2017) Thoracic temporal subtraction three dimensional computed tomography (3D-CT): screening for vertebral metastases of primary lung cancers. PLoS One 12(1):e0170309
19. Beg MF, Miller MI, Trouvé A, Younes L (2005) Computing large deformation metric mappings via geodesic flows of diffeomorphisms. Int J Comput Vis 61:139–157
20. Glaunès J, Qiu A, Miller MI, Younes L (2008) Large deformation diffeomorphic metric curve mapping. Int J Comput Vis 80:317–336
21. Dorfman DD, Berbaum KS, Metz CE (1992) Receiver operating characteristic rating analysis. Generalization to the population of readers and patients with the jackknife method. Invest Radiol 27(9):723–731
22. Chakraborty DP, Berbaum KS (2004) Observer studies involving detection and localization: modeling, analysis, and validation. Med Phys 31(8):2313–2330
23. Boardman LA, Peipert JF (1998) Screening and diagnostic testing. Clin Obstet Gynecol 41(2):267–274
24. Jemal A, Ward EM, Johnson CJ et al (2017) Annual report to the nation on the status of cancer, 1975-2014, featuring survival. J Natl Cancer Inst 109(9)
25. Reinbold WD, Wannenmacher M, Hodapp N, Adler CP (1989) Osteodensitometry of vertebral metastases after radiotherapy using quantitative computed tomography. Skeletal Radiol 18(7):517–521